Biogeotechnics 4 (2026) 100168

Contents lists available at ScienceDirect

Biogeotechnics

journal homepage: www.keaipublishing.com/en/journals/biogeotechnics/

Research Article

Role of *Trichoderma Virens* mycelium in enhancing erosion resistance of low plasticity silt

Joon Soo Park[a,1], Hai Lin[b,2,*], William M. Moe[b,3]

[a] GeoEngineers, Inc., 17425 NE Union Hill Road #250, Redmond, WA 98052, USA
[b] Department of Civil Engineering and Environmental Engineering, Louisiana State University, 3255 Patrick F. Taylor Hall, Baton Rouge, LA 70803, USA

ARTICLE INFO

Keywords:
Fungal mycelium
Erosion
Water dripping test
Soil water repellency

ABSTRACT

Conventional techniques for soil erosion control often rely on the use of cementing additives and coating agents to improve shear strength, minimize particle movement, and increase soil water repellency. These chemical agents, however, involve energy intensive production and treatment processes and can cause significant environmental impacts. Recent studies have demonstrated that fungal mycelium (a root-like three-dimensional structure of fungi) can extend through soil pores and secrete strong hydrophobic compounds, binding soil particles together and increasing soil water repellency at the soil surface. This study investigated the effect of fungal mycelium on the erosion resistance of a low plasticity silt for potential soil erosion mitigation. Water dripping tests were conducted on untreated and fungal-treated specimens under various conditions, including different fungal growth durations, void ratios, water dripping rates, and desiccation condition. Untreated specimen exhibited a 45% soil mass loss and 10.5 mm of erosion depth after one hour of water dripping. In contrast, fungal-treated specimens showed no loss of soil mass and 4–5 mm of erosion depths after four hours of water dripping. Furthermore, fungal mycelium remained effective in erosion resistance even after 30 days of desiccation at 60 °C.

1. Introduction

Soil erosion leads to significant environmental and economic consequences (Sartori et al., 2019). According to the National Resources Inventory (USDA, 2020), approximately 1.7 billion tons of cropland soil were lost due to erosion of wind and water between 2007 and 2017. Water-induced erosion can also trigger geotechnical failures, such as embankment collapse (Seed et al., 2008), bridge scour (Lagasse et al., 1995; Shirole & Holt, 1991), and slope stability failure (Abramson et al., 2001; Lawler, 1993).

Conventional techniques for soil erosion control often use cementing additives, such as cement and lime, to improve shear strength and minimize particle movements (Han, 2015). Recent research has also explored the treatment of chemical-based coating agents to increase soil water repellency and mitigate soil erosion, including wax (Bardet et al., 2015; Bardet et al., 2011), silane compounds (Byun et al., 2011; Chan & Lourenço, 2016; Daniels & Hourani, 2009; Keatts et al., 2018a; Ng & Lourenço, 2016), polytetrafluorethylene (PTFE) (Lee et al., 2015), and organic acids (González-Peñaloza et al., 2013; Subedi et al., 2012; Wijewardana et al., 2015). The use of cementing additives, however, involves high energy consumption and expensive and invasive earthworks (Andrew, 2019; Dejong et al., 2013; Fay et al., 2012; Karol, 2003). The application of chemical-based coating agents is also constrained by various limitations, including the hazardous nature of some coating materials (e.g., producing hydrogen chloride fumes when dimethyldichlorosilane reacts with water, Chan & Lourenço, 2016), the requirement for large quantities of coating chemicals (e.g., requiring high silane content for treating moist soil, Chan & Lourenço, 2016; Ng & Lourenço, 2016), and energy-intensive treatment process (e.g., requiring high temperature heating for wax coating, Bardet et al., 2015).

To develop environmentally friendly alternatives to those erosion control techniques, extensive research has explored several

* Corresponding author.
E-mail address: hailin1@lsu.edu (H. Lin).
[1] ORCID: https://orcid.org/0000-0003-3845-5767
[2] ORCID: https://orcid.org/0000-0002-1641-4588
[3] ORCID: https://orcid.org/0000-0002-9286-8004

https://doi.org/10.1016/j.bgtech.2025.100168
Received 23 December 2024; Received in revised form 11 February 2025; Accepted 27 February 2025
Available online 27 February 2025

microbiological processes, such as microbially induced carbonate precipitation (MICP) and enzyme induced carbonate precipitation (EICP) (Ghasemi & Montoya, 2022; Hamdan & Kavazanjian, 2016). This research explores the use of filamentous fungi to improve erosion resistance of soils. Recent research has demonstrated the ability of filamentous fungi to bind soil particles and increase soil water repellency (Park et al., 2023, 2025, Park, 2024; Salifu & El Mountassir, 2020; Salifu et al., 2021, Park, 2024; Zhang et al., 2023). Filamentous fungi can form a root-like three-dimensional fiber network in soils, known as fungal mycelium. Fungal mycelium can enmesh soil particles, produce extracellular polymeric substances (EPS), and induce mineral precipitation, which can bind and cement soil particles (Caesar-Tonthat, 2002; Chenu, 1989; Clough & Sutton, 1978; Daynes et al., 2012; Degens et al., 1996; Dorioz et al., 1993; Gadd, 2001; Lehmann & Rillig, 2015; Ritz & Young, 2004; Tisdall et al., 2012; Zhang et al., 2023). Furthermore, aerial mycelium (i.e., interfacial fungal mycelium between air and soil surface) can increase soil water repellency by secreting hydrophobic compounds (i.e., hydrophobins), resulting in reductions of water infiltration and hydraulic conductivity (Park et al., 2023; Salifu, 2019).

A few studies investigated the effect of fungal mycelium on sand erodibility for application in soil erosion mitigation (Salifu, 2019; Zhang et al., 2023). Salifu (2019) conducted impinging jet tests on untreated and *Pleurotus ostreatus* fungal-treated sand-lignocellulose mixture under incremental hydraulic head pressures applied every 60 minutes. During the initial 60 minutes under a hydraulic head of 50 mm, untreated specimens showed scour depth of 16–31 mm, while no scour was observed in fungal-treated specimens. The scour depth of untreated specimens increased by 11–21 mm for the following 60 minutes under 100 mm of hydraulic pressure, while the scour depth of fungal-treated specimens increased by only 6 mm. Additionally, Zhang et al. (2023) conducted scour resistance tests by using a rotating blade submerged in water above the sand specimens treated by *Pleurotus ostreatus*. At a rotation speed of 120 r/min, scour depth of 5.2 mm was observed at the edge of the specimen surface, while no scour was observed in the tests of fungal-treated specimens under rotation speeds at 120, 170, and 300 r/min. In both studies, the reduced erodibility in fungal-treated sand specimens was attributed to the particle binding by fungal mycelium attaching to and enmeshing sand particles and the increased soil water repellency due to the strong hydrophobicity of aerial mycelium. The influence of fungal mycelium on the erodibility of soil types other than sand, however, remains unexplored.

This study investigated the effect of fungal mycelium on the erodibility of a low plasticity silt. The low plasticity silt was treated with a nonpathogenic, nonparasitic, saprotrophic, and filamentous fungus, *Trichoderma virens* (ATCC 9645). Contact angle and water drop penetration time of fungal-treated silt were measured to assess the degree of water repellency. Water dripping tests were conducted on untreated and fungal-treated silt specimens under different conditions, including fungal growth durations, void ratios, water dripping rates, and desiccation conditions. The erosion profile of the specimens after water dripping tests were visualized using the Structure from Motion (SfM) technique. Furthermore, scanning electron microscopy (SEM) imaging was conducted to investigate the microscale morphology of fungal-treated silt specimens.

2. Materials and methods

2.1. Baton rouge silt

A silt was collected at the Accelerated Loading Facility of the Louisiana Transportation Research Center (LTRC), Baton Rouge, LA. This silt will be referred to as BR silt hereafter. The soil composition of BR silt was determined by performing sieve analysis and hydrometer test using an automated particle size analyzer (PARIO, Meter Group, Pullman, WA). BR silt is composed of 22% sand, 50% silt, and 28% clay and has the mean grain size (D_{50}) of 19 μm. Liquid limit and plasticity index of BR silt were measured as 33% and 17, respectively. Based on the results of grain size analysis and Atterberg limit test, BR silt was classified as low plasticity silt with some sand and clay (ML), according to the unified soil classification system (USCS). Before use, BR silt was oven-dried, pulverized, and autoclaved (15 min at 121 °C and 100 kPa). Autoclaving was intended to minimize the growth of other non-target microorganisms (e.g., bacteria, fungi, and mold), that may affect growth of *Trichoderma virens* fungal mycelium and its influence on erosion resistance of BR silt samples.

2.2. Fungal strain and nutrient solution

This study selected *Trichoderma virens* for BR silt treatment. *Trichoderma virens* is an aerobic, non-pathogenic, non-parasitic, saprotrophic (i.e., feeds on organic matter and releases nutrients to the environments), and filamentous fungus. The selection of *Trichoderma virens* is because it is a soil fungus with rapid growth rate (8.0–9.5 cm in diameter after 4 days) according to the American Type Culture Collection (ATCC). *Trichoderma virens* (ATCC 9645), obtained from the ATCC (Manassas, VA), was used to produce a stock culture of fungal spores as described by Park et al. (2023). The stock culture was distributed into sterile 2 mL cryogenic tubes (i.e., fungal spore suspension), which were stored in a freezer at –80 °C until use.

Potato dextrose broth (PDB) was employed as the liquid nutrient source for fungal growth. PDB was prepared by adding 24 g of granulated PDB (HiMedia, Kennett Square, PA) per liter of deionized water prior to autoclaving (15 min at 121 °C and 100 kPa). The PDB contains (per L) solubilized potato infusion (4 g) and dextrose (20 g). The pH of PDB is (5.1 ± 0.2) at 25 °C.

2.3. Specimen preparation

Test specimens were prepared in a sterile specimen cell, resulting in specimen dimensions of 80 mm in diameter and 50 mm in height (total volume = 250 cm^3). Fungal-treated specimens were prepared with targeted void ratios of 0.65, 0.7, and 0.75, corresponding to the dry densities of 1606, 1559, and 1514 kg/m^3, respectively. The void ratio of 0.65 was selected based on the experience of the previous study (Park et al., 2025), in which fungal-treated BR silt specimens with void ratio of 0.65 were found to exhibit improved mechanical properties compared to untreated specimens. Void ratios of 0.7 and 0.75 were selected to investigate the effect of additional void ratios on the erosion resistance of fungal-treated BR silt samples. Preliminary samples prepared with higher void ratios (e.g., 0.8) were found to be easily disturbed during extrusion from the specimen cell following sample preparation and were therefore not included in testing. BR silt (about 378 g to 397 g depending on the targeted void ratios) was mixed with PDB (about 68–75 mL) and fungal spore suspension (4 mL) to achieve a targeted degree of saturation of 0.7. This degree of saturation was selected to maintain an unsaturated state and ensure sufficient oxygen availability for the growth of fungal mycelium (Salifu, 2019). The specimens were then compacted in the specimen cell in five equal thickness layers. Each layer received forty blows from a metal tamper weighing 1 kg for specimens with a void ratio of 0.65 and forty and thirty blows from a metal tamper weighing 0.3 kg for specimens with void ratios of 0.7 and 0.75, respectively. The specimens were then carefully extruded, with the inner wall of the specimen cell spread with a thin layer of petroleum jelly for smooth extrusion. The specimens were then transferred into sterile food containers, which were then covered with Parafilm to minimize contamination. The specimens were then incubated in an incubator at 25 °C for fungal growth durations of 3, 5, and 10 days, respectively. Hereafter, the fungal-treated specimens with 3, 5, and 10 days of fungal growth durations will be referred to as FG3, FG5, and FG10 specimens. Fig. 1A–D show images of untreated, FG3, FG5, and FG10 specimens, respectively. As shown in Fig. 1B–D, thicker aerial mycelia covered a greater surface area of the fungal-treated specimens

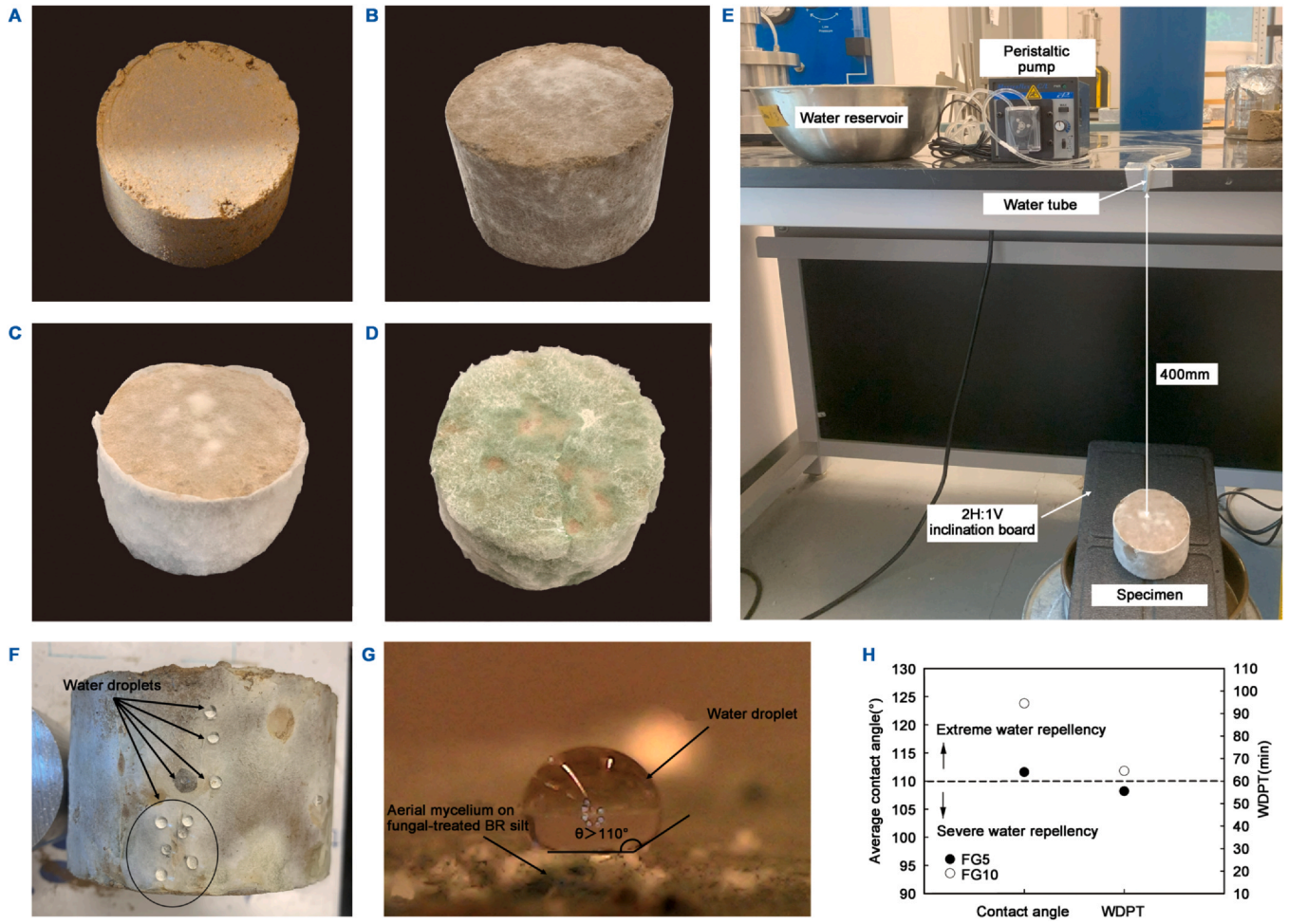

Fig. 1. Images of (**A**) untreated, (**B**) FG3, (**C**) FG5, and (**D**) FG10 specimens, and (**E**) test setup of Geelong drip test; (**F**) Image of water droplets on fungal-treated BR silt specimen surface; (**G**) Microscope image of a water droplet on fungal-treated BR silt with a contact angle higher than 110°; (**H**) Average contact angles and WDPTs of FG5 and FG10 specimens.

with longer fungal-growth durations. This indicates that the specimens with longer fungal growth durations exhibit higher fungal content. The fungal mycelial mass in the specimen could plausibly be estimated by loss on ignition method (i.e., heating the oven-dried specimen in a muffle furnace at 550 °C for 2 h to facilitate calculation of the difference in measured weights after oven-drying and heating in the muffle furnace. The fungal mass and contents within the fungal-treated specimens were not determined using this approach in the current study, however, as the variation of organic contents in the BR silt and differences in unconsumed organics from the PDA could significantly affect the fungal content measurements. An untreated specimen was prepared with a targeted void ratio of 0.65 following the same procedure as the fungal-treated specimens, except that PDB and fungal spore suspension were replaced with the same amount of deionized water.

2.4. Contact angle and water drop penetration time measurements

This study measured contact angle (interface angle between aerial mycelium and water droplet) and water drop penetration time (WDPT) of water droplets on fungal-treated BR silt to assess its degree of water repellency. FG5 and FG10 specimens with void ratio of 0.75 were prepared following the specimen preparation procedure as described in Section 2.3. After fungal growth durations, 20 water droplets of 10 μL were released from a height of 5 mm above the top and side surfaces of FG5 and FG10 specimens (Bachmann et al., 2000). Contact angles of the 20 water droplets were then measured following the procedure described in a previous study by the research team (Park et al., 2023). Images of water droplets were taken within 5 s after water droplet release using a 1000X-USB-Microscope Camera. The contact angles were estimated using the Low Bond Axisymmetric Drop Shape Analysis (LBADSA) in ImageJ software (Stalder et al., 2010; Salifu & El Mountassir, 2020). Furthermore, WDPT was also measured during the contact angle measurements. The time was recorded from the moment of water droplet release to the moment of full infiltration into the specimen. The average contact angle and WDPT of 20 water droplets were then used to classify the degrees of water repellency of fungal-treated sands according to the water repellency criterion provided by Doerr et al. (2006) as shown in Table 1.

2.5. Geelong drip test

The effect of fungal mycelium on the erodibility of BR silt was investigated using the Geelong drip test method. The Geelong method is a

Table 1
Water repellency criterion between the degree of water repellency, contact angle, and WDPT (after Doerr et al., 2006).

Degree of water repellency	Contact angle (°)	WDPT (s)
Hydrophilic	0	< 5
Slight	0–80	6–60
Moderate	80–110	61–600
Severe	N/A	601–3600
Extreme	> 110	> 3600

Table 2
Specimens and test conditions of Geelong drip tests.

Specimen type	After fungal growth				After desiccation		
	Fungal growth duration (days)	Void ratio	Water dripping rate (mL/h)	Dripping duration (h)	*Desiccation duration (days)	Water dripping rate (mL/h)	Dripping duration (h)
Untreated	-	0.65	300	1	-	-	-
FG3	3	0.65	300	4	-	-	-
FG5	5	0.65	300		30	300	4
	5	0.65	600		-		
	5	0.7	300		-	-	-
	5	0.75	300		-	-	-
FG10	10	0.65	300		30	300	4
	10	0.65	600		-		
	10	0.7	300		-	-	-
	10	0.75	300		-	-	-

* Desiccation duration indicates the period of desiccation in an oven at 60 °C, following the initial Geelong drip test.

New Zealand Standard method (NZS 4298) developed to assess the durability of earthen building materials against water-induced erosion (NZS, 2020). Geelong drip tests were conducted under various conditions, including fungal growth duration, void ratio, water dripping rate, dripping duration, and desiccation condition, as shown in Table 2.

In the Geelong drip test, water is dispensed at a regulated rate through a peristaltic pump from a height of 400 mm onto the specimen surface positioned at an inclination of 2 H:1 V (NZS, 2020), as shown in Fig. 1E. The outlet of the water tube with a diameter of 1.9 mm was fixed to the benchtop corner to minimize the dispersion of water drops. Water dripping rates of 300 mL/h and 600 mL/h were used in this study, corresponding to rainfall rates of 9.3 mm/h and 18.6 mm/h, respectively, as measured by an 8-inch standard rain gauge. Fungal-treated specimens were subjected to the Geelong drip test for 4 hours, while an untreated specimen was subjected to the Geelong drip test for 1 hour due to the soil mass loss by erosion during the test.

The Geelong drip test was also conducted on FG5 and FG10 specimens under desiccation condition. The goal of the drip tests under desiccation condition was to assess the durability of fungal mycelium against extreme heat and dry condition. The FG5 and FG10 specimens with void ratio of 0.65, initially tested with a water dripping rate of 300 mL/h, were subjected to desiccation for 30 days in an oven at 60 °C. After the desiccation, the degrees of saturation (S) of the FG5 and FG10 specimens were approximately 0.02. The FG5 and FG10 specimens were then subjected to the Geelong drip test at a water dripping rate of 300 mL/h for 4 hours.

After Geelong drip tests, Structure from Motion (SfM) technique was employed to visualize the resulting erosion profiles and estimate the erosion depths in specimens. SfM constructs a 3D point cloud, which is a discrete set of points representing the 3D shape of the specimen, by establishing correspondences between multiple and overlapping 2D images. For the SfM technique, 20–30 images of the specimens were randomly taken at different locations using a digital camera (Nikon D7100). To enhance the visibility of erosion in the images for SfM analysis, an LED spotlight (LED-6W dual Gooseneck illuminator, Amscope, Irvine, California) was directed toward the scour while taking the images. Visual SfM (Wu, 2013; Wu et al., 2011) software was employed to generate a 3D point cloud. A detailed procedure for operating VisualSfM can be found on the software's website. Subsequently, CloudCompare 2.13 (Dublin, Ireland) was utilized to process the 3D point cloud of specimens and measure the erosion depth, using the point picking tool in the software.

2.6. SEM imaging

SEM imaging was conducted to investigate the morphology of fungal-treated BR silt. After Geelong drip test, samples for SEM imaging were collected from FG5 and FG10 specimens. While the FG 5 specimen with void ratio of 0.65 was used for SEM imaging, FG 10 specimens with void ratios of 0.65, 0.7, and 0.75 were used. Samples were collected from three specific locations within the cylindrical specimens, the top surface, midsection (approximate 15 mm from the top and side surfaces), and center (25 mm from the top surface and 40 mm from the side surface). These samples will be referred to as top surface sample (TSS), midsection sample (MS), and center sample (CS). Samples were dried at 105 °C for at least 24 hours prior to SEM imaging. Samples were then subjected to sputter coating using platinum to prevent charging of the sample for high-quality imaging. SEM imaging was performed using a Quanta 3D Dual Beam SEM (FEI, Hillsboro, Oregon). Everhart-Thornley detector at an acceleration voltage of 10 kV and magnification ranging from 2500 to 5000× was used in the SEM imaging.

3. Results and discussions

3.1. Contact angle and water drop penetration time of fungal-treated BR silt

Contact angles could not be measured for untreated BR silt as water droplets infiltrated into the specimen within 1 s. This indicates untreated BR silt exhibited hydrophilic condition according to the water repellency criterion (i.e., WDPT $<$ 5 s, Table 1). However, the multiple water droplets stably remained on the side surface of FG10 specimen, as shown in Fig. 1F. Fig. 1G shows a microscope image of a water droplet on FG10 specimen with contact angle higher than 110 degrees. Fig. 1H shows the average contact angles and WDPTs of FG5 and FG10 specimens. Both FG5 and FG10 specimens exhibited average contact angles higher than 110°, indicating extreme water repellency. While FG5 specimen had an average WDPT slightly lower than 60 min, FG10 specimen had an average WDPT higher than 60 min. This classifies FG5 and FG10 specimens as severe and extreme water repellency, respectively, according to Table 1. FG10 specimen showed higher average values than FG5 specimen in both contact angle and WDPT measurements. This is attributed to the higher fungal content on the surfaces of FG10 specimen as confirmed by Fig. 1D, which increased the water repellency compared to FG5 specimen.

Previous studies (Park et al., 2023; Salifu & El Mountassir, 2020) also observed increases of water repellency in fungal-treated sands. Park et al. (2023) reported that the aerial mycelia of *Trichoderma virens* increased the degree of soil water repellency of Ottawa sands from hydrophilic to extreme and severe water repellency. Similarly, Salifu and El Mountassir (2020) treated a mixture of fine sand and lignocellulose with *Pleurotus ostreatus*, resulting in moderate to extreme water repellency. Both studies attributed these increases of water repellency to aerial mycelia secreting strong hydrophobic compounds in the air. However, Park et al. (2023) observed that the degree of water repellency inside Ottawa sand specimens remained as hydrophilic. This was attributed to the amphipathic characteristics of aerial mycelium,

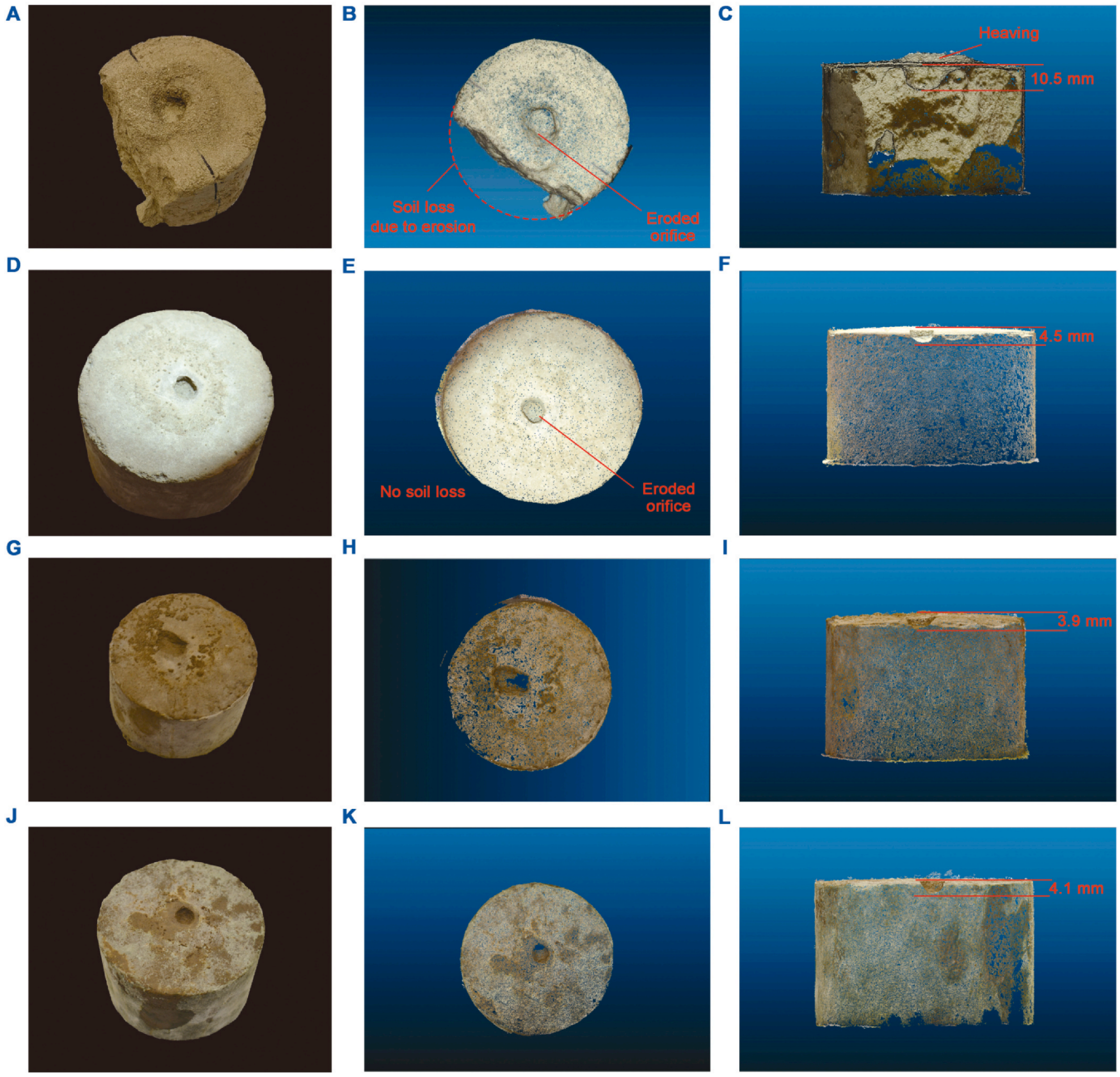

Fig. 2. Images and point clouds of untreated and fungal-treated specimens: (**A–C**) Untreated specimen; (**D–F**) FG3; (**G–I**) FG5; (**J–L**) FG10 specimens.

where hydrophobins in water are soluble and disperse (Wessels, 1996; Wösten & De Vocht, 2000; Wösten et al., 1994; Wösten et al., 1993, 1993).

3.2. Erosion depth of BR silt specimens with different fungal growth durations

Untreated and FG3, FG5, and FG10 specimens with void ratio of 0.65 underwent the Geelong drip test at water dripping rate of 300 mL/h. After the tests, point clouds of the specimens were produced using the SfM technique to visualize the erosion profile and estimate the erosion depths. The images and point clouds of the untreated and fungal-treated specimens are shown in Fig. 2. As shown in Fig. 2A–C, the untreated specimen exhibited 45% soil loss and an erosion depth of 10.5 mm at the center of the specimen. Also, soil heaving was observed near the eroded orifice. This indicates BR silt is unable to withstand 1 hour of rainfall with a rate of 9.3 mm/h (300 mL/h of water dripping rate simulates a rainfall rate of 9.3 mm/h). However, FG3, FG5, and FG10 specimens showed no soil loss (Fig. 2D–L), even after longer duration of water dripping (4 h) than untreated specimen (1 h).

Fig. 3A shows that the FG3, FG5, and FG10 specimens showed erosion depths of 4.5, 3.9, and 4 mm, respectively, which were lower than the erosion depth of 10.5 mm in the untreated specimen. The reduced erosion depth and improved erosion resistance of fungal-treated specimens can be attributed to the increased soil water repellency at the specimen surface (Fig. 1F–H), reduced hydraulic conductivity, and higher shear strength compared to untreated specimens. This is supported by the findings in Park et al. (2023) and Salifu et al. (2021) that fungal mycelia reduced water infiltration and hydraulic conductivity of soils by increasing soil water repellency on the soil surface and occupying the pore space in the soil matrix. Also, Park et al. (2025) reported that *T. virens* increased the shear strength of low-plasticity silt due to the increased capillary and physicochemical forces by fungal mycelia. Furthermore, Zhang et al. (2023) reported that the strong

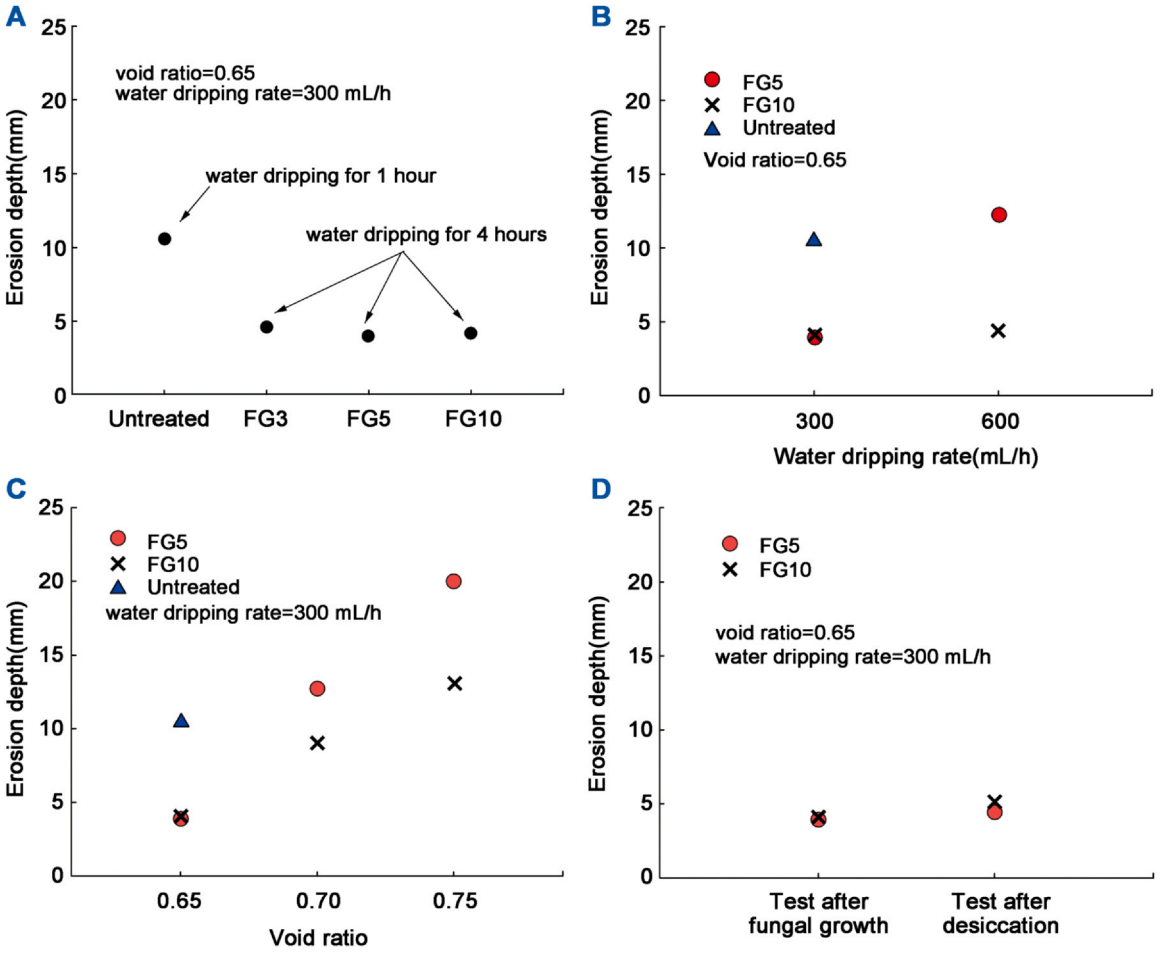

Fig. 3. Erosion depths of untreated, FG3, FG5, and FG10 specimens under various conditions: (**A**) Fungal growth durations; (**B**) Water dripping rates; (**C**) Void ratios; (**D**) Desiccated conditions.

hydrophobicity of aerial mycelium caused water to slip on the fungal mycelia surface, enhancing flow mobility. This means that the dropped water experienced increased ease of flow across the fungal-treated specimen surfaces, consequently mitigating water-induced shear stress acting on the specimen surface.

3.3. Erosion depths of FG5 and FG10 specimens under different water dripping rates

After tests conducted at a water dripping rate of 600 mL/h, both FG5 and FG10 specimens exhibited no soil loss (results not shown for conciseness) as compared to the soil loss of untreated specimen (Fig. 2A), indicating fungal-treated BR silt can withstand 4 hours of rainfall with a rate of 18.6 mm/h (600 mL/h of water dripping rate simulates a rainfall rate of 18.6 mm/h). The erosion depths of untreated, FG5, and FG10 specimens were compared at water dripping rates of 300 mL/h and 600 mL/h in Fig. 3B. The erosion depth of FG10 specimen slightly increased from 4 to 5 mm when the dripping rate increased from 300 to 600 mL/h. However, FG5 specimens showed a significant increase of erosion depth from 3.9 to 12.2 mm, which is higher than the erosion depth of untreated specimen (10.5 mm). The increase of erosion depth of FG5 specimens from 300 mL/h to 600 mL/h could be attributed to the lower amount of fungal mycelia in FG5 specimen as compared to FG 10 specimens, which made FG5 specimen unable to stabilize soil against higher rainfall rate.

3.4. Erosion depth of FG5 and FG10 specimens with different void ratios

Fig. 3C shows the erosion depths of untreated specimen with void ratio of 0.65 and FG5 and FG 10 specimens with void ratios of 0.65, 0.7, and 0.75. Since the untreated specimen with void ratio of 0.65 experienced significant soil loss, it was expected that untreated specimens with void ratios of 0.7 and 0.75 would experience more significant soil loss. Both FG5 and FG10 specimens showed increased erosion depth with increasing void ratio, indicating that the erosion resistance of fungal-treated BR silt reduced with the increasing void ratio. However, FG5 specimens showed a higher rate of increase in erosion depth with void ratio compared to FG10 specimens. The erosion depth of FG5 specimen increased from 3.9 to 20 mm with void ratio incrementing from 0.65 to 0.75, while those of FG10 specimens increased from 4 to 13 mm with the same increment of void ratio.

The test results of fungal-treated specimens with different water dripping rates and void ratios (Fig. 3B and C) show a trend that longer fungal growth duration resulted in a reduced rate of erosion depth increase with increasing water dripping rate and void ratio. This suggests that longer fungal growth durations may decrease the dependence of erosion resistance on soil void ratio and water dripping rate. The lower dependence of FG10 specimens on water dripping rate and soil void ratio may be due to the increased fungal content compared to the FG5 specimens as shown in Fig. 1C and D. The increased fungal content could increase water repellency on the surface and reduce hydraulic conductivity within the specimen. As discussed before, the fungal

contents of fungal-treated specimens were not measured. However, the observed higher fungal content of FG10 compared to FG5 can be supported by the findings in Park et al. (2023) that fungal-treated sands with longer fungal growth durations showed higher fungal contents, leading to more significant reductions of hydraulic conductivities due to increased soil water repellency and occupancy of pore space compared to those samples with shorter fungal growth durations.

3.5. Erosion depth of desiccated FG5 and FG10 specimens

Geelong drip tests were performed again on FG5 and FG10 specimens with void ratio of 0.65 after desiccation (desiccated fungal-treated specimens at 60 °C for 30 days following the initial Geelong drip test as shown in Table 2) to evaluate the durability of fungal mycelium treatment against extreme heat and dry condition. The erosion depths of FG5 and FG10 specimens are compared between the tests after fungal growth and desiccation in Fig. 3D. In the desiccation tests, the erosion depth of FG5 specimen increased from 3.9 to 4.5 mm, while that of FG10 specimen increased from 4 to 5 mm. This indicates that desiccation did not significantly increase the erosion depths of FG5 and FG10 specimens, although it might reduce the viability of fungal mycelium in the specimens. As discussed in the results of previous studies (Park et al., 2023; Salifu & El Mountassir, 2020), the degree of water repellency of fungal-treated sands increased from moderate to severe and extreme water repellency when the degree of saturation reduced from 1 to less than 0.1. Also, Park et al. (2025) reported that the magnitude of suction stress (attractive stress between soil particles) in fungal-treated BR silt increased by as much as 116 kPa with a reduction of degree of saturation from 0.7 to 0.13. This resulted in the increase of shear strength, which could improve erosion resistance of BR silt. Therefore, as the degree of saturation reduced from 0.7 to approximately 0.02 during the desiccation, the magnitude of suction stress and soil water repellency of FG5 and FG10 specimens increased, contributing to maintaining the erosion resistance after desiccation. The slight increases of erosion depths in the desiccation tests further suggest that fungal mycelia remain effective in improving erosion resistance even under extreme environments of high temperature and dry conditions.

3.6. Micro-scale morphology of fungal-treated BR silt

SEM images of FG5 and FG10 specimens are shown in Fig. 4. Fig. 4A–C show SEM images of the top surface sample (TSS), midsection

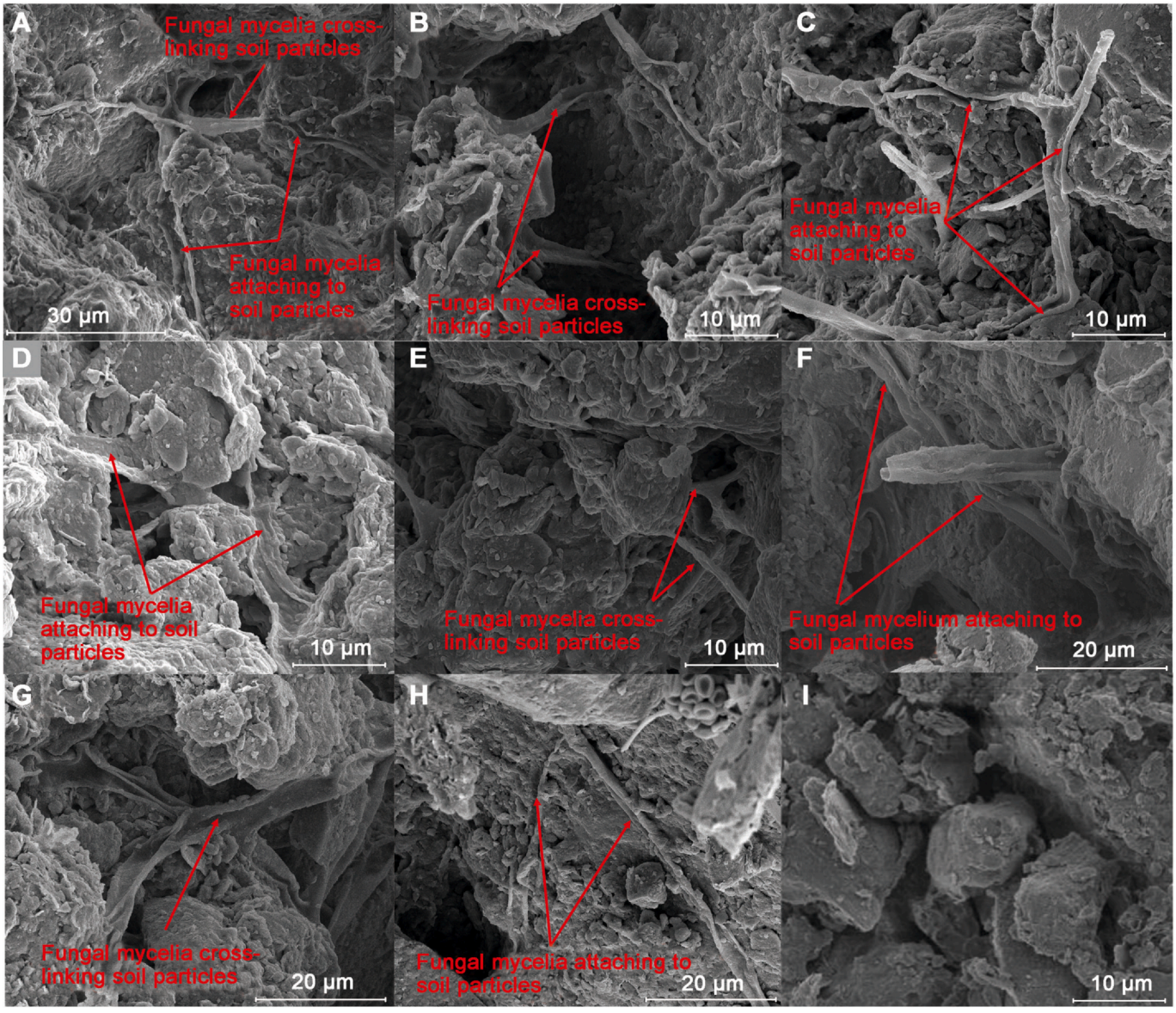

Fig. 4. SEM images of (**A**) TSS, (B) MS, and (**C**) CS of FG5 specimen with void ratio of 0.65; (**D**) TSS, (**E**) MS, and (**F**) CS of FG10 specimen with void ratio of 0.65; (**G**) CS of FG10 specimen with void ratio of 0.7; (**H**) CS of FG 10 specimen with void ratio of 0.75; and (**I**) untreated BR silt specimen.

sample (MS), and center sample (CS) in FG5 specimen with void ratio of 0.65, respectively. Also, Fig. 4D–F show SEM images of TSS, MS, and CS in FG10 specimen with void ratio of 0.65, respectively. While the SEM imaging was also performed for TSS, MS, and CS in FG 10 specimens with void ratios of 0.7 and 0.75, the SEM images of only CS in FG10 specimen with void ratio of 0.7 and 0.75 are shown in Fig. 4G and H for the sake of conciseness. Fig. 4I shows the untreated BR silt specimen.

Fungal mycelia attached to (Fig. 4A, C, D, F, and H) and cross-linked soil particles (Fig. 4A, B, E, and G) as compared to the untreated specimen (Fig. 4I), which could modify the pore structures and bind the soil particles in the BR silt specimens. The binding of fungal mycelium in BR silt may result from capillary and physicochemical interactions (e.g., van der Waals attraction, electrostatic interactions, and fungal osmosis) between soil particles, pore water, and fungal hyphae, as discussed in previous studies (Park et al., 2023, 2025). Therefore, the SEM images support the results in the Geelong drip tests that fungal mycelia improved erosion resistance of BR silt by modifying pore structures and binding soil particles.

It worth mentioning that the void ratio of BR silt samples could change after fungal growth as the pore space was occupied by fungal mycelia as shown in Fig. 4. The final void ratio is worth measuring as it could provide insights on the morphology and content of fungal mycelia in soil. However, the authors' lab does not have the equipment (e.g., pore size analyzer based on mercury intrusion, capillary flow, or gas adsorption, and X-Ray Computed Tomography) to measure the final void ratio, which requires further investigation in the future.

Fungal mycelia were present in all samples of the FG5 and FG10 specimens, regardless of their locations and void ratios (Fig. 4). This indicates that fungal mycelium can grow and extend throughout the pore space of BR silt samples. This finding could be supported by the study of Rebata-Landa and Santamarina (2006), which characterized the bacterial activity in soil based on soil particle size and depth, which could be applied to assess the behavior of fungal mycelia in BR silt samples. The diameter of the fungal hyphae observed in SEM images ranged from 1 to 6.7 μm. Considering the size of the fungal mycelia and the mean size of 19 μm for BR silt particles, it can be inferred that the activity of fungal mycelia in the BR silt specimens is likely "active and motile" as described by Rebata-Landa and Santamarina (2006).

Park et al. (2025) reported that fungal mycelia were able to grow in BR silt and silica silt, which have mean grain sizes of 19 μm and 11 μm, respectively. This growth resulted in increased unconfined compressive strength, tensile strength, and suction stress. However, the fungal mycelium could not grow in kaolinite due to the small pore size (mean grain size of 4 μm) of kaolinite and therefore did not increase the unconfined compressive strength of kaolinite.

4. Conclusion

This study conducted water repellency and water dripping tests to investigate the effect of fungal mycelium on the erosion resistance of low plasticity silt. Contact angle and water drop penetration time of fungal-treated silt were measured to assess the degree of water repellency. To investigate the erodibility of silt after fungal treatment, water dripping tests were conducted on untreated and fungal-treated silt specimens under different test and specimen conditions, including fungal growth durations, void ratios, water dripping rates, and desiccation condition. The following conclusions are drawn from the results presented in this paper.

1. Fungal mycelia significantly increased contact angles and WDPTs of fungal-treated BR silt, which indicated the specimen surface was modified from hydrophilic to severe and extreme water repellency after fungal treatment.
2. Fungal mycelium can improve soil erosion resistance. As compared to untreated BR silt that exhibited 45% soil mass loss during one hour of Geelong drip test, the fungal-treated specimens did not show any significant soil loss during the four hours of the drip test. Also, for specimens prepared at void ratio of 0.65 and tested at water dripping rate of 300 mL/h, the erosion depths of the fungal-treated specimens were significantly lower (4–5 mm) than that of the untreated specimen (10.5 mm). The improved erosion resistance was attributed to fungal mycelia increasing soil water repellency, reducing water infiltration and hydraulic conductivity of soil, and improving soil strength.
3. The water dripping rate and void ratio can affect erosion resistance of fungal-treated BR silt. Erosion depth increased from 3.9 to 12.2 mm for FG5 specimens with void ratio of 0.65 when water dripping rate increased from 300 to 600 mL/h. Also, erosion depth increased from 3.9 to 20 mm with void ratio increased from 0.65 to 0.75 for FG5 specimens subjected to 300 mL/h water dripping rate.
4. Increasing fungal growth duration led to higher fungal content, resulting in higher erosion resistance of fungal-treated specimens. This is because higher fungal content led to higher soil water repellency, lower hydraulic conductivity, and higher soil shear strength. The results also imply that a higher fungal content can reduce the dependence of erosion resistance on soil void ratio and water dripping rate.
5. After 30 days of desiccation at 60 °C, the erosion depth of the silt specimens increased by only 1 mm. Although desiccation may reduce the viability of fungal mycelium in the specimens, the test results suggest that fungal mycelia remain effective in improving erosion resistance of silt after desiccation.

CRediT authorship contribution statement

Moe William M.: Conceptualization, Writing – review & editing. **Lin Hai:** Writing – review & editing, Supervision, Resources, Project administration, Methodology, Funding acquisition, Conceptualization. **Park Joon Soo:** Writing – original draft, Visualization, Validation, Methodology, Investigation, Formal analysis, Data curation, Conceptualization.

Data availability

The data used to support the findings of this study are available from the corresponding author upon reasonable request.

Declaration of Competing Interest

The authors declare the following financial interests/personal relationships which may be considered as potential competing interests: Hai Lin reports financial support was provided by State of Louisiana Board of Regents. Hai Lin reports financial support was provided by National Science Foundation. Hai Lin is the Associate Editor for Biogeotechnics, he was not involved in the editorial review or the decision to publish this article. The other authors declare that they have no known competing financial interests or personal relationships that could have appeared to influence the work reported in this paper.

Acknowledgement

The authors would like to acknowledge the support of the Louisiana Board of Regents Research Competitiveness Subprogram under Grant No. 039A-19, the transportation infrastructure precast innovation center (TRANS-IPIC) under grant No. 69A3552348333, and the National Science Foundation under Award No. 2339618. The authors would also like to thank the staff of the LSU Shared Instrumentation Facility for assistance with SEM imaging.

References

Abramson, L. W., Lee, T. S., Sharma, S., & Boyce, G. M. (2001). *Slope stability and stabilization methods.* John Wiley and Sons.

Andrew, R. M. (2019). Global CO2 emissions from cement production, 1928-2018. *Earth System Science Data, 11*(4), 1675–1710. https://doi.org/10.5194/ESSD-11-1675-2019

Bachmann, J., Ellies, A., & Hartge, K. H. (2000). Development and application of a new sessile drop contact angle method to assess soil water repellency. *Journal of Hydrology, 231–232*, 66–75. https://doi.org/10.1016/S0022-1694(00)00184-0

Bardet, J.P., Jesmani, M., Jabbari, N., & Lourenco, S.D.N. (2015). Permeability and compressibility of wax-coated sands. Https://Doi.Org/10.1680/Geot.13.P.118, *64*(5), 341–350. https://doi.org/10.1680/GEOT.13.P.118.

Bardet, J.-P., Jesmani, M., & Jabbari, N. (2011). Effects of compaction on shear strength of wax-coated sandy soils. *The Electronic Journal of Geotechnical Engineering, 16*, 451–461.

Byun, Y. H., Khoa Tran, M., Yun, T. S., & Lee, J. S. (2011). Strength and stiffness characteristics of unsaturated hydrophobic granular Media. *Geotechnical Testing Journal, 35*(1), 193–200. https://doi.org/10.1520/GTJ103650

Caesar-Tonthat, T. C. (2002). Soil binding properties of mucilage produced by a basidiomycete fungus in a model system. *Mycological Research, 106*(8), 930–937. https://doi.org/10.1017/S0953756202006330

Chan, C. S. H., & Lourenço, S. D. N. (2016). Comparison of three silane compounds to impart water repellency in an industrial sand. *Géotechnique Letters, 6*(4), 263–266. https://doi.org/10.1680/JGELE.16.00097

Chenu, C. (1989). Influence of a fungal polysaccharide, scleroglucan, on clay microstructures. *Soil Biology and Biochemistry, 21*(2), 299–305. https://doi.org/10.1016/0038-0717(89)90108-9

Clough, K. S., & Sutton, J. C. (1978). Direct observation of fungal aggregates in sand dune soil. *Canadian Journal of Microbiology, 24*(3), 333–335. https://doi.org/10.1139/m78-056

Daniels, J. L., & Hourani, M. S. (2009). Soil improvement with organo-silane. In *Advances in Ground improvement. Geotechnical Special Publication, 188*, 217–224.

Daynes, C. N., Zhang, N., Saleeba, J. A., & McGee, P. A. (2012). Soil aggregates formed in vitro by saprotrophic Trichocomaceae have transient water-stability. *Soil Biology and Biochemistry, 48*, 151–161. https://doi.org/10.1016/j.soilbio.2012.01.010

Degens, B. P., Sparling, G. P., & Abbott, L. K. (1996). Increasing the length of hyphae in a sandy soil increases the amount of water-stable aggregates. *Applied Soil Ecology, 3*(2), 149–159. https://doi.org/10.1016/0929-1393(95)00074-7

Dejong, J. T., Soga, K., Kavazanjian, E., Burns, S., Van Paassen, L. A., AL Qabany, A., Aydilek, A., Bang, S. S., Burbank, M., Caslake, L. F., Chen, C. Y., Cheng, X., Chu, J., Ciurli, S., Esnault-Filet, A., Fauriel, S., Hamdan, N., Hata, T., Inagaki, Y., & Weaver, T. (2013). Biogeochemical processes and geotechnical applications: Progress, opportunities and challenges. *Geotechnique, 63*(4), 287–301. https://doi.org/10.1680/geot.SIP13.P.017

Doerr, S. H., Shakesby, R. A., Dekker, L. W., & Ritsema, C. J. (2006). Occurrence, prediction and hydrological effects of water repellency amongst major soil and land-use types in a humid temperate climate. *European Journal of Soil Science, 57*(5), 741–754. https://doi.org/10.1111/j.1365-2389 .2006.00818.x

Dorioz, J. M., Robert, M., & Chenu, C. (1993). The role of roots, fungi and bacteria on clay particle organization. An experimental approach. *Geoderma, 56*(1–4), 179–194. https://doi.org/10.1016/0016-7061(93)90109-X

Fay, L., Akin, M., & Xianming, S. (2012). *Cost-effective and sustainable road slope stabilization and erosion control.* Washington D.C: Transportation Research Board.

Gadd, G. M. (2001). *Fungi in bioremediation.* Cambridge University Presshttps://doi.org/10.1017/CBO9780511541780

Ghasemi, P., & Montoya, B. M. (2022). Field implementation of microbially induced calcium carbonate precipitation for surface erosion reduction of a coastal plain sandy slope. *Journal of Geotechnical and Geoenvironmental Engineering, 148*(9), Article 04022071. https://doi.org/10.1061/(ASCE)GT.1943-5606.0002836

González-Peñaloza, F. A., Zavala, L. M., Jordán, A., Bellinfante, N., Bárcenas-Moreno, G., Mataix-Solera, J., Granged, A. J. P., Granja-Martins, F. M., & Neto-Paixão, H. M. (2013). Water repellency as conditioned by particle size and drying in hydrophobized sand. *Geoderma, 209–210*, 31–40. https://doi.org/10.1016/J.GEODERMA.2013.05.022

Hamdan, N., & Kavazanjian, E. (2016). Enzyme-induced carbonate mineral precipitation for fugitive dust control. *Géotechnique, 66*(7), 546–555. https://doi.org/10.1680/JGEOT.15.P.168

Han, J. (2015). *Principles and practice of ground improvement.* Johns and Wiley.

Karol, R. H. (2003). *Chemical grouting and soil stabilization.* Crc Press.

Keatts, M. I., Daniels, J. L., Langley, W. G., Pando, M. A., & Ogunro, V. O. (2018a). Apparent contact angle and water entry head measurements for organo-silane modified sand and coal fly ash. *Journal of Geotechnical and Geoenvironmental Engineering, 144*(6), Article 04018030. https://doi.org/10.1061/(ASCE)GT.1943-5606.0001887

Lagasse, P., Schall, J., Johnson, F., Richardson, E., Assistants, T., Arneson, L., Dunn, C., Harrison, L., Morris, J. L., Pagan, J., Trent, R., Waddoups, A., Richardson, J., Zevenbergen, L., Young, G. K., & Atayee, A. T. (1995). Stream stability at highway structures. *Federal Highway Administration*.

Lawler, D. M. (1993). The measurement of river bank erosion and lateral channel change: A review. *Earth Surface Processes and Landforms, 18*(9), 777–821. https://doi.org/10.1002/ESP.3290180905

Lee, C., Yang, H.-J., Yun, T. S., Choi, Y., & Yang, S. (2015). Water-entry pressure and friction angle in an artificially synthesized water-repellent silty soil. *Vadose Zone Journal, 14*(4), 1–9. https://doi.org/10.2136/VZJ2014.08.0106

Lehmann, A., & Rillig, M. C. (2015). Understanding mechanisms of soil biota involvement in soil aggregation: A way forward with saprobic fungi? *Soil Biology and Biochemistry, 88*, 298–302. https://doi.org/10.1016/j.soilbio.2015.06.006

Ng, S. H. Y., & Lourenço, S. D. N. (2016). Conditions to induce water repellency in soils with dimethyldichlorosilane. *Géotechnique, 66*(5), 441–444. https://doi.org/10.1680/JGEOT.15.T.025

NZS (2020). *NZS 4297 Engineering design of earth buildings.* Standards New Zealand.

Park, J. S., Lin, H., Chen, E., Alqrinawi, H., Dong, Y., & Moe, W. M. (2025). Mechanical properties of fine-grained soils treated with fungal mycelium of trichoderma virens. *Journal of Geotechnical and Geoenvironmental Engineering*. https://doi.org/10.1061/JGGEFK/GTENG-12745

Park, J.S. (2024). Soil improvement using fungal mycelium of trichoderma virens and construction techniques of mud dauber. LSU Doctoral Dissertations.

Park, J. S., Lin, H., Moe, W. M., & Salifu, E. (2023). Hydraulic properties of sands treated with fungal mycelium of trichoderma virens. *Journal of Geotechnical and Geoenvironmental Engineering, 149*(11), Article 04023093. https://doi.org/10.1061/JGGEFK.GTENG-11111

Rebata-Landa, V., & Santamarina, J. C. (2006). Mechanical limits to microbial activity in deep sediments. *Geochemistry, Geophysics, Geosystems, 7*(11), 1–12. https://doi.org/10.1029/2006GC001355

Ritz, K., & Young, I. M. (2004). Interactions between soil structure and fungi. *Mycologist, 18*(2), 52–59. https://doi.org/10.1017/S0269915X04002010

Salifu, E. (2019). Engineering fungal-mycelia for soil improvement. University of Strathclyde.

Salifu, E., & El Mountassir, G. (2020). Fungal-induced water repellency in sand. *Géotechnique*, 1–25. https://doi.org/10.1680/jgeot.19.p.341

Salifu, E., El Mountassir, G., Minto, J. M., & Tarantino, A. (2021). Hydraulic behaviour of fungal treated sand. *Geomechanics for Energy and the Environment*Article 100258. https://doi.org/10.1016/J.GETE.2021.100258

Sartori, M., Philippidis, G., Ferrari, E., Borrelli, P., Lugato, E., Montanarella, L., & Panagos, P. (2019). A linkage between the biophysical and the economic: Assessing the global market impacts of soil erosion. *Land Use Policy, 86*, 299–312. https://doi.org/10.1016/J.LANDUSEPOL.2019.05.014

Seed, R. B., Bea, R. G., Abdelmalak, R. I., Athanasopoulos-Zekkos, A., Boutwell, G. P., Briaud, J.-L., Cheung, C., Cobos-Roa, D., Ehrensing, L., Govindasamy, A. V., Harder, L. F., Inkabi, K. S., Nicks, J., Pestana, J. M., Porter, J., Rhee, K., Riemer, M. F., Rogers, J. D., Storesund, R., & Wartman, J. (2008). New Orleans and Hurricane Katrina. I: Introduction, overview, and the east flank. *Journal of Geotechnical and Geoenvironmental Engineering, 134*(5), 701–717.

Shirole, A. M., & Holt, R. C. (1991). Planning for a comprehensive bridge safety assurance program. *Transport Research Record, 1290*, 137–142.

Stalder, A. F., Melchior, T., Müller, M., Sage, D., Blu, T., & Unser, M. (2010). Low-bond axisymmetric drop shape analysis for surface tension and contact angle measurements of sessile drops. *Colloids and Surfaces, 364*(1-3), 72–81. https://doi.org/10.1016/j.colsurfa.2010.04.040

Subedi, S., Kawamoto, K., Jayarathna, L., Vithanage, M., Moldrup, P., Jonge, L. W. de, & Komatsu, T. (2012). Characterizing time-dependent contact angles for sands hydrophobized with oleic and stearic acids. *Vadose Zone Journal, 11*(1), https://doi.org/10.2136/VZJ2011.0055

Tisdall, J. M., Nelson, S. E., Wilkinson, K. G., Smith, S. E., & McKenzie, B. M. (2012). Stabilisation of soil against wind erosion by six saprotrophic fungi. *Soil Biology and Biochemistry, 50*, 134–141. https://doi.org/10.1016/j.soilbio.2012.02.035

U.S. Department of Agriculture (2020). *2017 national resources inventory summary report.* Washington D.C: National Resources Conservation Service.

Wessels, J. G. H. (1996). Hydrophobins: Proteins that change the nature of the fungal surface. *Advances in Microbial Physiology, 38*, 1–45. https://doi.org/10.1016/S0065-2911(08)60154-X

Wijewardana, N. S., Kawamoto, K., Moldrup, P., Komatsu, T., Kurukulasuriya, L. C., & Priyankara, N. H. (2015). Characterization of water repellency for hydrophobized grains with different geometries and sizes. *Environmental Earth Sciences, 74*(7), 5525–5539. https://doi.org/10.1007/S12665-015-4565-6/TABLES/3

Wösten, H. A. B., & De Vocht, M. L. (2000). Hydrophobins, the fungal coat unravelled. *Biochimica et Biophysica Acta (BBA) - Reviews on Biomembranes, 1469*(2), 79–86. https://doi.org/10.1016/S0304-4157(00)00002-2

Wösten, H. A. B., Schuren, F. H. J., & Wessels, J. G. H. (1994). Interfacial self-assembly of a hydrophobin into an amphipathic protein membrane mediates fungal attachment to hydrophobic surfaces. *The EMBO Journal, 13*(24), 5848. https://doi.org/10.1002/j.1460-2075.1994.tb06929.x

Wösten, H. A. B., Van Wetter, M. A., Lugones, L. G., Van der Mei, H. C., Busscher, H. J., & Wessels, J. G. H. (1999). How a fungus escapes the water to grow into the air. *Current Biology, 9*(2), 85–88. https://doi.org/10.1016/S0960-9822(99)80019-0

Wosten, H. A. B., De Vries, O. M. H., & Wessels, J. G. H. (1993). Interfacial self-assembly of a fungal hydrophobin into a hydrophobic rodlet layer. *The Plant Cell, 5*(11), 1567–1574. https://doi.org/10.1105/TPC.5.11.1567

Wu, C. (2013). Towards linear-time incremental structure from motion. Proceedings - 2013 International Conference on 3D Vision, 3DV 2013, 127–134. https://doi.org/10.1109/3DV.2013.25.

Wu, C., Agarwal, S., Curless, B., & Seitz, S.M. (2011). Multicore bundle adjustment. Proceedings of the IEEE Computer Society Conference on Computer Vision and Pattern Recognition, 3057–3064. https://doi.org/10.1109/CVPR.2011.5995552.

Zhang, X., Fan, X., Wang, C., & Yu, X. (2023). A novel method to improve the soil erosion resistance with fungi. *Acta Geotechnica, 18*(5), 2827–2845. https://doi.org/10.1007/S11440-022-01673-8/METRICS